Journal of Inclusion Phenomena and Molecular Recognition in Chemistry **21**: 185–213, 1995.

Coordination Chemistry in Zeolites

DIRK E. De VOS, PETER. P. KNOPS-GERRITS, RUDY F. PARTON, BERT M. WECKHUYSEN, PETER A. JACOBS and ROBERT A. SCHOONHEYDT

1. Introduction

Zeolites are relatively rigid inorganic matrices with cavities and channels of molecular dimensions and of different sizes and shapes. Transition metal ion (TMI) complexes in molecular sieves have three main characteristics: (1) the complexes have strongly reduced mobility with respect to their solution mobility and deactivating aggregations may be avoided; (2) complexation with extra-lattice ligands is in competition with complexation to lattice oxygens. Unusual complexes can be synthesized, depending on the relative coordinating strength of the structural oxygens and the extra-lattice ligands; and (3) shape-selectivity is not only operative on the size and shape of complexes which can be synthesized, but is also evident in the catalytic properties of the occluded complexes. Research on coordination chemistry in zeolites started around 1970 and most of the early work has been summarized by Lunsford [1].

The field can be subdivided into three areas: (1) Complexes which are smaller than the free diameters of the channels and windows giving access to the cavities. These complexes can be absorbed from a solution phase into the zeolite or they can be synthesized via absorption of the ligand into a TMI-exchanged zeolite; (2) Complexes which are larger than the free diameters of the channels and windows of the zeolite. Such complexes must be synthesized in situ, i.e., by absorption of the ligands into the TMI-loaded zeolite, or by synthesis of the ligand in the zeolite in the presence of the TMI; (3) Complexes which serve as fingerprints of the oxidation state, the location, and the coordination environment of the TMI. An example of the latter group are the CO and NO complexes. In this chapter, the first two areas will be covered with an emphasis on the synthesis and spectroscopic signatures of the encapsulated complexes.

The overwhelming majority of reported complexes have been immobilized in the supercages of zeolite Y; the site nomenclature of which is recalled in Figure 1. In the supercages two types of sites are of interest: site II (on the oxygen six-ring) and site III or III' (on the four-ring of oxygens). The former are also the preferential sites of TMI in zeolite A.

The spectroscopic signatures of Cu^{2+}, Co^{2+}, Ni^{2+}, and Cr^{2+}, coordinated to the lattice oxygens, are given in Table 1 [2,3]. The ions coordinated to six-rings have one free

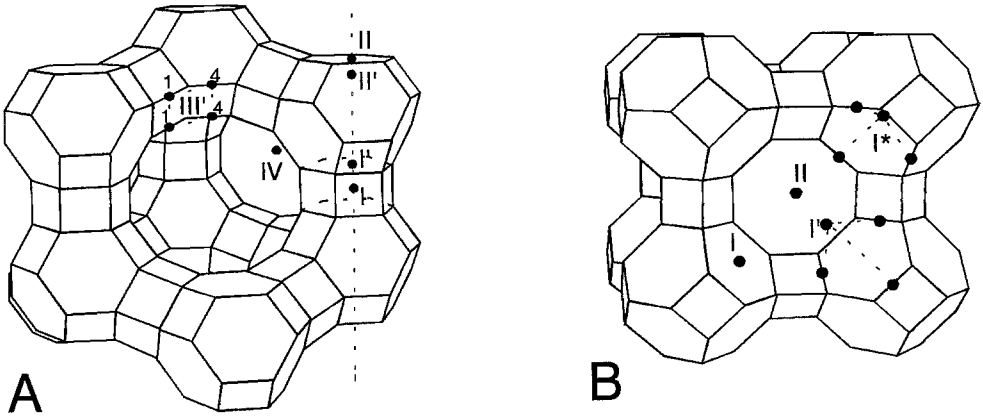

Figure 1. Structures of (A) zeolite Y and (B) zeolite A; different cation sites are indicated with Roman numerals. Arabic numerals indicate positions of structural oxygen atoms.

Table 1. Spectroscopic signatures of transition metal ions coordinated to lattice oxygens in zeolites.*

	site	*d-d* absorption bands	$g_{\|\|}$	$A_{\|\|}$	$g_{\perp}$	$A_{\perp}$
zeolite A						
Cr^{2+}	I	12000, 17000				
Co^{2+}		6000, 15000-20000, 25000				
Ni^{2+}		4500, 9100, 22800				
Cu^{2+}		10400, 12200, 15000	2.40	12.6	2.07	0.2
zeolites X,Y						
Ni^{2+}	I	6100-6400, 19000-20000				
	I',II	4900, 9300, 21500-23500				
Cu^{2+}	I'	10700, 12900, 14800	2.34	15.7	2.07	1.9
	II	10400, 12400, 14700	2.39	12.4	2.07	1.3

* Absorption frequencies in cm^{-1}; hyperfine constants in mT.

coordination site and readily accept one extra-lattice ligand to form pseudo-tetrahedral complexes.

Such is the case for weak ligands such as olefins, as shown by Klier and co-workers for Co-A [3]. Stronger ligands favorably compete with lattice oxygens for coordination sites. If enough ligands are offered in the cavities and channels, and if space is available, full coordination with these extra-lattice ligands is possible, giving (pseudo-)octahedral complexes. In such cases, the zeolite acts as an anionic solvent. Complexes may undergo distortion to match the size of the complex to the size and shape of the zeolite cavities.

2. Synthesis of Complexes in Zeolites

Figure 2 summarizes the different methods used for synthesis of complexes in zeolites. Two main routes can be followed: (1) synthesis starting from a preformed complex and (2) complex assembly inside the zeolite. The choice of the route depends on the zeolite, TMI, and on the ligands.

Synthesis with a preformed complex	↔	Complex assembly in the zeolite
→ Exchange of a preformed complex		→ with solvent :
		non-aqueous medium
		aqueous medium
→ Template synthesis		
		→ without solvent :
		in situ ligand synthesis
→ Anchorage of a complex precursor		gas phase absorption
		impregnation with liquid ligand

Figure 2. Overview of the different synthesis routes for complexes in zeolites.

2.1 SYNTHESIS WITH A PREFORMED COMPLEX

2.1.1 Exchange of Preformed Complexes

Direct ion-exchange of preformed cationic complexes depends on the resistance of the zeolite to acid or base and on the dimensions of the ring of oxygen atoms defining the zeolite windows and channels. Therefore, this method is only appropriate if: (a) the complexes are stable; (b) the solutions have no extreme pH; and (c) the complexes are small enough to enter into the zeolite. Thus, only (octahedral) complexes with ligands such as H_2O, NH_3, and some aliphatic amines may be exchanged without steric

limitations. For acid solutions, e.g., of Cr^{3+} and Fe^{3+}, the contact time must be very short to avoid zeolite lattice destruction.

2.1.2 Template Synthesis

Preformed complexes can also be used as templates during the synthesis of zeolites [4,5] (see also Chapter 6 in this volume). There are two important requirements which must be fulfilled for this route: (i) The complexes must be stable under synthesis conditions. For example, in the synthesis of zeolite Y, the complex must be stable in basic conditions and at high temperature, while for $AlPO_4$ synthesis it must be stable in acidic conditions. (ii) The complex must be soluble and randomly dispersed in the synthesis mixture.

2.1.3 Anchorage of a Complex Precursor

When heterobinuclear organometallics are absorbed into zeolites, an oxophilic metal may anchor the complex through reaction with the zeolite surface. For example, $Me_3SnMn(CO)_5$ and $Cl_2(THF)GeMo(CO)_5$ can react with acidic zeolites at elevated temperatures; volatile products such as methane or hydrogen chloride are removed [6]. Sample preparation involves mixing of a dehydrated acidic zeolite with the complexes in an organic medium under an inert atmosphere.

2.2 COMPLEX ASSEMBLY INSIDE THE ZEOLITE

Complexes, unstable under ion-exchange or zeolite synthesis conditions, can be synthesized by assembly in the zeolite. This method usually starts by ion-exchange of the zeolite with the desired TMI, followed by introduction of the ligand. This can be done in the absence or in the presence of a solvent. A condition for complex formation is that the complexation constant of the TMI with the lattice oxygens be lower than that with the added ligand.

2.2.1 Assembly without Solvent

Three synthesis routes can be envisaged: (1) gas phase absorption of the ligand; (2) impregnation of the zeolite by the liquid ligand; and (3) in situ ligand synthesis. Gas phase absorption of ligands, like NH_3, H_2O, CO, and NO can be done easily. The only restrictions are that the ligands be small enough to enter the pores or channels and have a vapor pressure at room temperature. For impregnation, the ligand must have a low enough melting point. In situ ligand synthesis needs diffusion of the ligand precursor into the zeolite to form, in situ, a stable ligand, which is able to chelate the TMI.

2.2.2 *Assembly with Solvent*

Complex assembly inside zeolites using solvents can be performed both in aqueous and non-aqueous media. The choice of solvent depends on the solubility of the ligand, the pore architecture of the zeolite material, and the affinity of the solvent for the zeolite. The latter is determined by the Si/Al ratio. Indeed, Si-rich zeolites are hydrophobic and an increasing Al content raises the hydrophilicity.

3. Coordination of Transition Metal Ions with Monodentate Ligands

The state of the art of complexes between TMIs and monodentate ligands in zeolites was reviewed in 1985 by Mortier and Schoonheydt [2]. In this chapter, we take this review as a starting point to give a general overview of the fundamental early work and recent progress. A whole series of monodentate ligands have been used as complexants of TMI in zeolites: H_2O, RNH_2 (R=H, CH_3, or $CH_3CH_2CH_2$), pyridine, picoline, PR_3 (R=CH_3, Ph), CH_3NC, and CN^-, and results are now reviewed below.

3.1 WATER COMPLEXES

TMI-H_2O complexes are easily introduced into zeolites by ion-exchange and can be characterized by their typical *d-d* absorption bands. Upon drying, one (or more) H_2O ligands in the first coordination sphere of the TMI may be replaced by surface oxygens. High temperature treatment can result in complete dehydration and migration of the TMI to the cation exchange sites in the smaller zeolite cages.

Re-absorption of H_2O into a dehydrated zeolite causes back-migration of the cations to the large cages, where hexa-aquo complexes can be re-formed. However, this process may be slow and incomplete.

The absorption-desorption scheme can be represented as:

$$[TMI(H_2O)_6]^{n+} \rightleftarrows [TMI(O_{lat})_p(H_2O)_q]^{n+} \rightleftarrows [TMI(O_{lat})_r]^{n+} \quad (1)$$

where both (p+q), $r \leq 6$. In zeolites A, X, and Y, controlled absorption and desorption of water occurs via an intermediate pseudo-tetrahedral complex [7]. In this complex, the TMI is coordinated to three oxygens of a six-ring (site II) and one water molecule (p=3, q=1). Coordination of two water molecules, one on either side of the six-ring, has also been suggested.

3.2 ISONITRILE COMPLEXES

Vansant and Lunsford prepared Co(II)-isonitrile complexes in zeolite Y [8]. The gaseous

ligand was absorbed into the Co,Na-Y zeolite after a high-temperature dehydration. This treatment makes the Co(II) migrate to sites in the small cages of the zeolite. Although the CH_3NC certainly has no access to these sites, the Co cation smoothly returns to the faujasite supercages to form various isonitrile complexes. The symmetries of the low-spin Co(II) species, tetragonal six-coordinated, and square-pyramidal five-coordinated, were deduced from the X- and Q-band EPR spectra.

3.3 N-BASE COMPLEXES

A whole range of monodentate ligands, such as primary amines, pyridine, and picolines, has been used for designing TMI-complexes in zeolites. Especially for the aliphatic amines, complexation is in competition with protonation of the ligand by residual acidic protons of the TMI-loaded zeolites; however, protonation can be minimized by careful exchange of TMI and by gradual dehydration prior to ligand absorption.

3.3.1 Complexes with Ammonia and Alkylamines

Only in the case of 4*d* and 5*d* TMI is direct exchange of, e.g., $[Pd(NH_3)_4]^{2+}$ and $[Pt(NH_3)_4]^{2+}$ possible [9]. Ammonia complexes of 3*d* TMI are prepared by gas-phase absorption of NH_3 into ion-exchanged and dehydrated zeolites. This may lead to six-coordinated complexes, but sometimes unsaturated $[TMI(NH_3)_m]^{2+}$ complexes are formed, with $m < 6$. For example, square-planar $[Cu(NH_3)_4]^{2+}$ is smoothly formed upon absorption of ammonia into copper zeolites, as revealed by the analysis of the EPR spectra [10,11]. The chemistry of these ammonia complexes is somewhat similar to that of the aquo complexes. Thus, upon controlled desorption, intermediate $[TMI(O_{lat})_3(NH_3)]^{n+}$ complexes are formed, similar to the pseudo-tetrahedral mono-aquo complexes [7].

In an analogous way, Co(II)ammonia-complexes were made in zeolite Y [12]. These complexes are themselves EPR invisible, but their oxygen adducts show characteristic EPR spectra. Thus, zeolite occluded $[Co(NH_3)_5]^{2+}$ interacts with molecular oxygen to form mononuclear $[Co(III)(NH_3)_5O_2^-]$, which is slowly converted into the dinuclear-peroxo complex.

Similar complexes are formed on Co,Na-Y zeolite with CH_3NH_2 and $CH_3CH_2CH_2NH_2$ [13]. The larger dimensions of these complexes restrict their mobility. As a consequence, formation of dimeric complexes, which occurs with NH_3, is not observed for complexes of alkylamines.

3.3.2 Complexes with Aromatic Amines

Furthermore, TMI-complexes with aromatic amines, such as pyridine and picoline, have

been prepared and characterized [14-18]. For example, planar $[Cu(pyridine)_4]^{2+}$ was prepared by absorption of pyridine vapor into a Cu,Na-Y zeolite [14,15]. The pyridine ligands have also been attached covalently to the zeolite surface by a silylation procedure. Such immobilized Cu-complexes have been used as catalysts for the oxidative coupling of 2,6-dimethylphenol [16].

Instead of pyridine, α-, β-, or γ-picoline may be used. Yamada used $[Cu(acac)_2]$-impregnated zeolites as the precursor material in this type of synthesis (acac = acetylacetonate) [17,18]. Formally, the complexation reaction can be viewed as an intrazeolitic exchange of non-framework ligands. Surface acidity is thought to facilitate the replacement of the anionic acetylacetonate by picoline.

3.4 PHOSPHINE COMPLEXES

Small monodentate phosphines, such as PMe_3, are very reactive molecules. Any complexation of TMI in zeolites with PMe_3, via gas-phase absorption of the latter, is in competition with reaction with surface oxygen atoms, hydroxyl groups, or residual water [19]. Phosphines are strongly chemisorbed on zeolites, with formation of P-O bonds. Heating is necessary to accelerate the reaction with the TMI. Mostly, the pseudo-tetrahedral high-spin $[TMI(O_l)_3(PMe_3)]^{n+}$ is formed [20,21]. Only in the presence of excess PMe_3, low-spin complexes of Co^{2+} or Ni^{2+} are detected, such as the trigonal bipyramidal $[Ni(PMe_3)_5]^{2+}$ [22,23]. With more bulky ligands, such as $P(Me)_2(C_6H_5)$, only pseudo-tetrahedral complexes can be synthesized [21].

In view of the importance of sorption, it is not surprising that the Si/Al ratio affects the result of the complexation. In Co,Na-Y zeolites, pseudo-tetrahedral Co^{2+} complexes are formed, but phosphine chemisorption on CoNa-X zeolites is so strong that tertiary phosphine complexes are not even detected [21].

3.5 CYANIDE COMPLEXES

The $[TMI^{n+}(CN^-)_m]^{(m-n)-}$ complexes are the only anionic coordination compounds yet occluded in zeolite cages [24-27]. The negative charge of the CN^- ligand necessitates special synthesis procedures. The best results were obtained by impregnation of dehydrated zeolites with methanolic NaCN solutions, although irreversible oxidation of, e.g., Co and Fe to the trivalent-state, is a major side-reaction [24,25].

The formation of low-spin Co(II) complexes and Co(II)-superoxo species on Co,Na-Y zeolites was evidenced by the EPR spectra [25,26]. There is, however, uncertainty concerning the number of CN^- ligands surrounding Co^{2+}. Both four- and five-coordination occurs and the monovalent zeolitic cations, such as Cs^+, seem to influence the complexation stoichiometry [27].

4. Coordination of Transition Metal Ions with Bi- or Polydentate Ligands

4.1 COMPLEXES OF ALIPHATIC POLYAMINES

4.1.1. Complexes of ethylenediamine (en)

a) Complexes with Cu(II)

The formation of complexes between zeolitic Cu(II) and en was studied in both aqueous media and in dehydrated zeolites [28]. As discussed previously, direct aqueous exchange of preformed cationic complexes requires high stability constants. This permits one to work in an aqueous solution with a minimal ligand excess. $[Cu(en)_2]^{2+}$ is an ideal case, as $K_1 = 10^{10.7}$ and $K_2 = 10^{9.3}$, giving an overall stability constant $\beta_2 = 10^{20}$ for :

$$[Cu(H_2O)_6]^{2+} + 2\,en \rightleftarrows [Cu(en)_2(H_2O)_2]^{2+} + 4\,H_2O. \quad (2)$$

In the supercages of zeolites Na-X and Na-Y, the equilibrium is shifted to the right for the *mono*-complex and to the left for the *bis*-complex, giving a stabilization and a destabilization, respectively. This effect is more pronounced on Na-X with its lower Si/Al ratio.

The prevalence of the *mono*-complex on Na-X may be a consequence of the higher negative surface charge density of this zeolite. It is, however, doubtful whether the lattice oxygen atoms can really compete with en for Cu(II). On the dehydrated zeolites Cu,Na-X and Cu,Na-Y, en absorption results in formation of *tris*-complexes. Apparently, even on X zeolites, the affinity of the lattice oxygens for Cu(II) is substantially lower than that of en. The larger apparent stability of the *mono*-complex on zeolite Na-X, therefore, is more likely due to a change in the protonation equilibrium for en :

$$en + H_2O \rightleftarrows enH^+ + OH^-. \quad (3)$$

Inside a Na-X supercage, the H_2O/Na^+ ratio is only about 3. The resulting strong polarization of the water molecules results in a higher acidity. Therefore, less en is available in its unprotonated form and the complexation equilibrium is shifted towards the *mono*-adduct.

b) Complexes with Co(II)

En uptake by dry Co,Na-Y zeolite is fast, but formation of the *tris*-complex may require heating and depends on the availability and mobility of the Co(II) ions. Low loadings of Co(II) tend to disfavor full complexation, while blocking of hidden sites with La^{3+}, accelerates full chelation [29].

The complexation of Co(II) by en is much stronger than that by monoamines. This

implies that, if one intends to use the system for O_2 binding, an evacuation treatment is needed to create a vacancy in the Co(II) coordination sphere [29,30]. There is, however, considerable debate on what the actual coordination around the active, O_2 binding Co(II) complex in en loaded Co(II) zeolites may be. Reflectance spectroscopy evidences the simultaneous presence of *mono-*, *bis-* and *tris*-complexes. An average number of two en ligands per Co(II), determined by gravimetry, seems optimal for O_2 binding [29]. The absence of an EPR low-spin Co(II) signal rules out a square-planar, *trans*-geometry for the *bis*-$[Co(en)_2]^{2+}$ complexes. Alternatives are a *cis*-$[Co(en)_2]^{2+}$ complex with four N donors, or a five-coordinate complex containing three en molecules, one of which acts as a monodentate ligand [31].

Oxygen binding results primarily in a $[Co(III)(en)_2 \cdot O_2^-]$ superoxo complex. The mononuclear nature of this compound was established not only by the EPR spectrum, but also by the energy of the charge transfer bands (Co(III) $\rightarrow O_2^-$ and $O_2^- \rightarrow$ Co(III)) in the reflectance spectrum [29]. In spite of the limited mobility of these complexes, deactivation occurs through formation of dimers. These dimers were identified by the higher energies for the charge transfer bands in the reflectance spectrum [29]. Use of the frequencies of these bands for excitation in resonance Raman spectroscopy results in a strongly enhanced intensity of, e.g., Co-O and O-O vibrations. In this way, the presence of monobridged-peroxo and, after H_2O infusion, of dibridged-peroxo-hydroxo complexes was established [31]:

$$[Co(en)_2]^{2+} + [Co(en)_2 \cdot O_2]^{2+} \rightarrow [Co(en)_2 \cdot O_2 \cdot Co(en)_2]^{4+} \quad (4)$$

$$[Co(en)_2 \cdot O_2 \cdot Co(en)_2] + H_2O \rightarrow [Co(en)_2 \cdot O_2(OH) \cdot Co(en)_2]^{3+} + H^+. \quad (5)$$

c) Complexes with other TMI

Howe and Lunsford reported complexation of Ni(II) and Mn(II) by en in zeolite Y and proved chelation by IR spectroscopy [32]. Especially $[Mn(II)(en)_2]^{2+}$-Na-Y has an enhanced activity in catalytic catechol oxidation by molecular oxygen.

4.1.2 Complexes with tetren

The use of tetren constitutes an extension of the prior work with amines and diamines. Tetren was absorbed aerobically from a 1 M aqueous solution on hydrated Co,Na-Y and Co,Na-A zeolites [33]. On Na-A, mononuclear superoxo complexes were observed in EPR and Raman spectra, but in Na-Y the reaction proceeds to peroxo Co(III) dimers:

(Na-A) $[Co(H_2O)_6]^{2+}$ + tetren + $O_2 \rightarrow [Co(tetren) \cdot O_2]^{2+} + 6\,H_2O$ (6)

(Na-Y) $[Co(tetren) \cdot O_2]^{2+} + [Co(tetren)]^{2+} \rightarrow [Co(tetren) \cdot O_2 \cdot Co(tetren)]^{4+}$. (7)

This difference was attributed to the steric constraints imposed by the small α-cage windows of Na-A, which inhibit reaction between the monomeric Co(II) complexes. It is, however, unclear whether the zeolite is stable in the synthesis conditions, as the pH of the aqueous tetren solution exceeds 13.

The oxygen binding affinity of zeolite A confined $[Co(tetren)]^{2+}$ is lower than that of $[Co(bpy)(terpy)]^{2+}$-Y and similar to that of [Co(SALEN)(py)]-Y. This is remarkable as in aqueous solution $[Co(tetren)]^{2+}$ has one of the highest O_2 affinities known for a Co(II) compound. The low O_2 affinity of the zeolite encapsulated complex was ascribed, by Dutta, to the hydrated state of the $[Co(tetren)]^{2+}$-Y zeolite [33]; the filling of the zeolite pores with water strongly decreases the access of O_2 to the active complex (see Chapters 6 and 8 of this volume for more details of this area).

4.2 DIMETHYLGLYOXIME COMPLEXES

The absorption of dimethylglyoxime ($dmgH_2$) into Na-X zeolites, partially exchanged with Co(II) or Ni(II), mostly yields a mixture of different species [34-37]. With Co(II) for instance, proposed speciations include $[Co(II)(dmgH)(O_l)_2]$ (with a distorted tetrahedral geometry), square-planar $[Co(II)(dmgH)_2]$, $[Co(II)(dmgH)_2(H_2O)_2]$ (a tetragonally distorted octahedron), and $[Co(III)(dmgH)_2(H_2O)O_2^-]$ (an octahedral superoxo complex) [34]. The first step in the complexation is the formation of a mixed chelate:

$$[Co(O_l)_3(H_2O)] + dmgH_2 \rightarrow [Co(O_l)_2(dmgH)] + H_3O^+ \quad (8)$$

where dmgH is the *mono*-anion of $dmgH_2$. The assignment is mainly based on UV-Vis spectroscopy [35] and is logical in view of the pronounced tendency of the Na-X surface to retain the cations or produce mixed chelates, as noted above for en and phosphine complex formation. XPS measurements support this proposition, as the absorption of $dmgH_2$ into Co,Na-Y does not change significantly the Co(II) binding energies [36]. However, for at least part of the Co(II), the reaction proceeds directly to the low-spin, four-coordinated Co(II) complex [34]:

$$Co(II) + 2\,dmgH_2 \rightarrow [Co(dmgH)_2] + 2\,H^+. \quad (9)$$

Two different types of this complex, a planar one and a distorted planar one, were identified by very well-resolved EPR spectra. Exposure of these square-planar Co(II) complexes to O_2 does not result in Co-O_2 formation, as O_2 binding to planar complexes requires axial base coordination *trans* to the O_2 binding site. H_2O infusion is sufficient to change the electronic structure of the complex and thus promotes O_2 binding:

$$[Co(dmgH)_2] + 2\,H_2O \rightarrow [Co(dmgH)_2(H_2O)_2] \quad (10)$$

$$[Co(dmgH)_2(H_2O)_2] + O_2 \rightarrow [Co(dmgH)_2(H_2O)\cdot O_2] + H_2O. \quad (11)$$

The EPR spectrum of $[Co(dmgH)_2(H_2O)_2]$ is that of a tetragonally distorted Co^{2+} complex. Reversibility of the O_2 sorption on the complex was not demonstrated.

For Ni(II), the complexation also seems to be a multistep process, since only after H_2O infusion on a $dmgH_2$ loaded Ni,Na-Y are appreciable changes in the XPS Ni(II) binding energies observable [36]. The addition of H_2O may be necessary to promote the cation mobility during the complexation process. XPS is also useful in following the spin-state of the Ni(II) cations, as Ni(II) paramagnetism gives rise to satellite peaks in the XPS measurements. A decrease of the intensity of these peaks upon $dmgH_2$ complex formation indicates that at least part of the Ni(II) has become diamagnetic. XPS thus provides an alternative for measurements of magnetic susceptibility, which, in the zeolitic medium, are strongly complicated by multi-speciation and the presence of Fe impurities.

In some cases, it was observed that reaction between $dmgH_2$ and TMI-exchanged zeolites led to cleavage of Na-X crystals, as monitored by electron microscopy [37], or to migration of the cations to the outer crystal surface, as detected by XPS measurements [36].

4.3 COMPLEXES WITH BIPYRIDINE, TERPYRIDINE, AND ANALOGS

This group of materials was originally devised by Lunsford and co-workers [38-44]. Potential applications of these encapsulation compounds include light energy storage and air separation [44,45]. Moreover, zeolite Na-X occluded [Gd(III)(8-hydroxyquinoline)$_2$]$^{1+}$ has been used as a magnetic resonance imaging contrast agent [46]. Catalytic applications are lacking until now, but optimism is warranted in view of the recent progress in homogeneous catalysis with bpy complexes.

In the patent literature, claims are given for ZSM-5 synthesis with [Ru(*o*-phenanthroline)$_3$Cl$_2$] and [Fe(bpy)$_3$(ClO$_4$)$_2$] [47]. These complexes are stable enough to be used as templates, but, because of their 1.2 nm diameter, they can only reside at the intersection of two perpendicular channels of the MFI lattice. As the obtained ZSM-5 was of low crystallinity, it is doubtful whether this approach merits further investigation. Better results are obtained when the complexes are assembled inside the zeolites.

4.3.1 Copper complexes

Formation of $[Cu(bpy)]^{2+}$ in zeolite Y was reported by De Wilde and Lunsford [38]. The 1:1 stoichiometry is a direct result of the synthetic approach. Zeolite Y was stirred in an aqueous solution of 2,2'-bipyridinium chloride and was subsequently exchanged with Cu(II). At the very small loading used (1 Cu(II) per 50 supercages), only *mono*

$[Cu(bpy)]^{2+}$ is formed. This was proved by the axially symmetric EPR spectrum with a five line superhyperfine structure, due to two equivalent nitrogen atoms. It was claimed that $[Cu(bpy)]^{2+}$ is not coordinated to lattice oxygens, but the insensitivity of the EPR parameters to dehydration suggests the opposite. Due to the low Cu(II) content a relatively large amount of free bipyridinium cations remain in the zeolite.

This synthetic approach is unique to Cu(II). In all other reports, the ligand is absorbed into metal-containing, dehydrated zeolites, resulting in formation of *bis*- or *tris*-complexes.

4.3.2 Ruthenium and iron complexes

Absorption of bpy into Ru^{3+} or $[Ru(NH_3)_6]^{3+}$ exchanged Na-Y yields *bis*- or *tris*-bpy complexes. The result of the synthesis depends on the metal-ligand stoichiometry and on the choice of the complexation temperature. *Bis*-complexes are selectively formed at 90° C with a 2:1 bpy:Ru stoichiometry [48]; however, at a 3:1 bpy:Ru stoichiometry and at 200° C, *tris*-complexes are formed as depicted in Figure 3 [39,40]. Generally Ru is reduced to its divalent state during synthesis, possibly by one of the following reactions [40]:

$$2\ Ru(III) + 8\ bpy \rightarrow 2\ [Ru(II)(bpy)_3]^{2+} + C_{20}H_{14}N_4 + 2\ H^+ \quad (12)$$

$$2\ [Ru(III)(NH_3)_6]^{3+} + 6\ bpy \rightarrow 2\ [Ru(II)(bpy)_3]^{2+} + N_2H_4 + 2\ NH_4^+ + 8\ NH_3 \quad (13)$$

$$6\ [Ru(III)(NH_3)_6]^{3+} + 18\ bpy \rightarrow 6\ [Ru(II)(bpy)_3]^{2+} + N_2 + 6\ NH_4^+ + 28\ NH_3. \quad (14)$$

The *bis*-$[Ru(II)(bpy)_2]^{2+}$ species is easily identified by its MLCT absorption at 488 nm [48]. A supplementary band at 606 nm was ascribed to lattice coordinated [(Al)Si-O-$Ru(bpy)_2(H_2O)$]. The assignment is based on the spectral similarity with the dinuclear $[(bpy)_2(H_2O)RuORu(H_2O)(bpy)_2]^{4+}$, which absorbs at 640 nm [49]. Apparently, the encapsulation in the zeolite cage prevents formation of the dinuclear complex; the free coordination sites are taken up by the lattice oxygen atoms. The assignment was confirmed by resonance Raman spectroscopy; the only difference between the spectra of the mononuclear zeolitic compound and the dinuclear crystalline compound is observed in the stretching modes of the Si-O-Ru and Ru-O-Ru bonds.

A general problem for *bis*-complexes of bidentate ligands is whether the complexes assume a *cis*- or a *trans*-geometry. For dissolved *bis*-bpy complexes, the *cis*-geometry is favored, but bulky axial ligands induce the *trans*-configuration [49]. The effect of zeolite encapsulation on the geometry is still unclear and may be worth looking at.

In the synthesis of the *tris*-$[Ru(II)(bpy)_3]^{2+}$ species, more than 80% of the total Ru can be transformed into the desired complex [39]. In order to investigate the location of the complexes, a sample, synthesized by the in situ method, was compared to a Na-Y sample which was impregnated with $[Ru(II)(bpy)_3]^{2+}$. XPS data proved that in the latter case the

complex surface concentration is much higher than in the former case. This proves that for the in situ sample, complexation is largely confined to the zeolite cages.

Kincaid et al. [48] prepared $[Ru(II)(bpy)_2(bpz)]^{2+}$-Y and $[Ru(II)(bpy)_2(dmb)]^{2+}$-Y by heating a mixture of $[Ru(II)(bpy)_2]^{2+}$-Y and the desired ligand (bpz or dmb) at 200° C. This method constitutes an elegant two-step approach to the preparation of mixed complexes in zeolites. However, the zeolite cage size prevents incorporation of larger

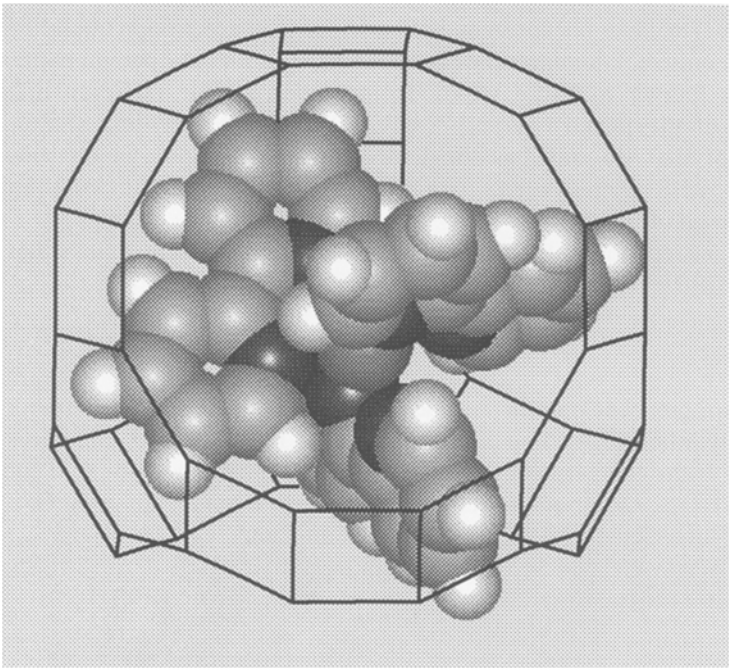

Figure 3. $[Ru(II)(bpy)_3]^{2+}$, occluded inside a zeolite Y supercage.

complexes. For instance, $[Ru(II)(bpz)_2(bpy)]^{2+}$ and $[Ru(II)(dmb)_2(bpy)]^{2+}$ cannot be made by this procedure.

Encapsulation of $[Ru(II)(bpy)_3]^{2+}$ in Na-Y strongly affects the luminescence properties of this complex [39,45,50]. The optimal conditions for emission by zeolite occluded complexes are low-loading, low content of paramagnetic impurities, and absence of oxygen.

In zeolites, *concentration* quenching occurs by resonance energy transfer from the excited complex to its neighbors. *Oxygen* quenching gives singlet oxygen and superoxide ions. *Water* causes quenching, when the ligand-attached hydrogen atoms assist in radiationless transitions. However, at high water loadings, the water molecules form an isolating mantle between the complexes and cause an increase of the emission intensity.

Dehydration of $[Ru(II)(bpy)_3]^{2+}$-Y results in a reduction of the rotational mobility of

the complex. The π-π^* bipyridine transition, the MLCT band, and the ^{3}CT emission band are all blue-shifted (from 285, 460 and 620 to 278, 449, and 586 nm, respectively). The ^{3}CT lifetime decay was fitted with a bi-exponential model, with lifetimes of 440 ns and 98 ns. However, this bi-exponential decay model does not exclude a multi-exponential model. Indeed, dehydration results in direct interaction of the complex with the surface; as a result, the complexes are all in slightly different environments.

An increase of the complex loading causes a red shift of the MLCT and reduces the ^{3}CT lifetime. The latter phenomenon is clearly due to concentration quenching.

In zeolites, only ^{3}CT luminescence is observed. In solution, thermal population of the ^{3}dd state is known to cause photodecomposition of the complex by deligation. Entrapment of the $[Ru(II)L_nL'_{3-n}]^{2+}$ complexes (L=bpy; L'=bpz or dpm) prevents population of the ^{3}dd state, as the Ru-N bond elongation (which should lead to deligation) is sterically restricted. As a result, the room temperature lifetime of the ^{3}CT state is increased [48].

An important reaction in the photocatalytic splitting of water is the water oxidation, e.g., by $[Ru(III)(bpy)_3]^{3+}$ [40]:

$$[Ru(III)(bpy)_3]^{3+} + OH^- \rightarrow [Ru(III)(bpy)_3]^{2+} + {}^1/_4\, O_2 + {}^1/_2\, H_2O. \quad (15)$$

The reaction proceeds only in well-defined pH ranges. Under *alkaline* conditions, a covalently hydrated bipyridine ligand is thought to be formed. This results in the formation of hydrogen peroxide, which is further oxidized to O_2 by two equivalents of $[Ru(III)(bpy)_3]^{3+}$. Under *acidic* conditions, H_2O_2 is not a precursor to O_2; the oxygen atoms remain associated with the Ru complex throughout:

$$[Ru(III)bpy_3]^{3+} + H_2O \rightarrow [Ru(II)bpy_3(OH^\bullet)]^{2+} + H^+ \quad (16)$$

$$[Ru(II)bpy_3(OH^\bullet)]^{2+} + [Ru(III)bpy_3]^{3+} \rightarrow [Ru(II)bpy_3(OH^\bullet)]^{3+} + [Ru(II)bpy_3]^{2+} \quad (17)$$

$$[Ru(III)bpy_3(OH^\bullet)]^{3+} \rightarrow [Ru(III)bpy_3O]^{2+} + H^+ \quad (18)$$

$$[Ru(III)bpy_3(OH^\bullet)]^{2+} + [Ru(III)bpy_3O]^{2+} \rightarrow 2\,[Ru(II)bpy_3]^{2+} + H^+ + O_2. \quad (19)$$

Upon zeolite entrapment, $[Ru(III)(bpy)_3]^{3+}$ remains reactive toward water. Evolution of oxygen is, however, not observed, although there is some evidence for formation of $OH^\bullet$ radicals. Lunsford et al. [40] have ascribed the lack of oxygen production to a pH effect. The effective pH in the zeolite is unknown, but it may well fall inside a range which is not suited for oxygen evolution.

In bpy-loaded Fe(II)-Y, several species were identified by Mössbauer spectroscopy [41]. The characteristics of the most intense signal correspond to those of the well-known octahedral, low-spin $[Fe(II)(bpy)_3]^{2+}$, which is probably situated near the center of the Na-Y supercage. A weaker Mössbauer doublet seems to correspond to a low-spin Fe(II) species with a coordination number greater than 6. In this complex, the Fe cation

is probably located at site IV (in the center of the twelve-membered ring of the cage window), where it is π-bonded to the ligands of two $[Fe(II)(bpy)_3]^{2+}$ complexes in adjacent supercages (see Figure 4). Finally, uncomplexed high-spin Fe(III) is observed, especially when the loading exceeds one Fe(II) per supercage.

Upon exposure of bpy-loaded Fe(II)-Y to chlorine, encapsulated $[Fe(II)(bpy)_3]^{2+}$ is largely oxidized to $[Fe(III)(bpy)_3]^{3+}$. The *g* values of the EPR spectrum of the oxidized sample are indeed indicative of a low-spin, axially symmetric $(t_{2g})^5$ complex.

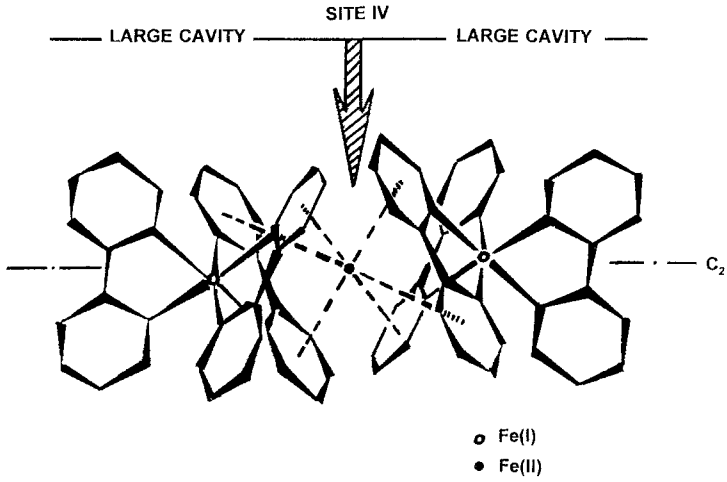

Figure 4. Model of low-spin Fe(II) at site IV in bpy loaded Fe(II)-Y. Fe is π-bonded to the ligands of two $[Fe(bpy)_3]^{2+}$ complexes in neighboring supercages (after Quayle et al., see reference [41] ; copyright *ACS.*).

4.3.3 Cobalt Complexes

$[Co(bpy)_3]^{2+}$-Y and $[Co(terpy)_2]^{2+}$-Y are easily obtained by solid-state reaction between dehydrated Co,Na-Y and bpy or terpy [42,43]. The spin-multiplicity of these complexes is variable. At 77 K, the EPR spectrum shows an 8-line hyperfine structure, which is ascribed to the low-spin complex. As the temperature is increased, the EPR spectrum gradually vanishes, due to the short relaxation time of the high-spin form [42]:

$$^2E \text{ } (low\text{-}spin) \quad \rightleftarrows \quad ^4T \text{ } (high\text{-}spin)$$

For $[Co(bpy)_3]^{2+}$, this equilibrium is considerably shifted to the left in the zeolite Y supercage. This was ascribed to steric constraints, which force the bpy ligands closer to

the Co(II) ion.

These six-coordinated complexes are unable to bind O_2. However, when a bpy-terpy mixture is used for Co,Na-Y impregnation, the mixed, oxygen-binding [Co(bpy)-(terpy)]$^{2+}$ can be obtained in fair yields [43]. The zeolitic [Co(III)(bpy)(terpy)·O_2^-]$^{2+}$ adduct is stable in oxygen up to 343 K. The [Co(bpy)(terpy)]$^{2+}$ content of the zeolite was maximized by optimization of the reactant stoichiometry and by variation of the monovalent cations on the zeolite. When Co(II), bpy, and terpy are introduced into Li-Y in a 1:2.5:2 ratio, an efficient system is obtained for separation of dry air into O_2 and N_2 [44].

4.4 SCHIFF-BASE COMPLEXES

4.4.1 Co(II) Complexes

Herron first proposed the use of the Schiff base ligand $SALENH_2$ for the formation of oxygen activating Co(II) centers within zeolite Y [51]. The synthesis is based on the "flexible-ligand" principle: the ligand is unfolded and twists its way through the metal exchanged zeolite. The metallo-SALEN complexes which are formed cannot pass through the 12-membered rings of the supercage. As the ligand is a weak bifunctional acid, the resulting complex is electroneutral:

$$Co(II) + SALENH_2 \rightarrow [Co(SALEN)] + 2\,H^+. \quad (20)$$

The final Soxhlet extraction only removes the excess ligand. The non-extractability of the neutral chelates indicates that they are retained in the zeolite by spatial restrictions alone; hence, these complexes are truly entrapped species. However, some leaching of Co(II) from the outer zeolite layers was demonstrated by XPS. A molecular graphics picture of [Co(SALEN)] complexes in a Y-type zeolite is shown in Figure 5.

Pyridine treatment of [Co(SALEN)],Na-Y results in the formation of an EPR detectable superoxo species. The observation of this species is a strong proof of the simultaneous, intrazeolitic coordination of Co(II) by SALEN and pyridine:

$$[Co(SALEN)] + \text{pyridine} + O_2 \rightarrow [Co(SALEN)\cdot\text{pyridine}\cdot O_2]. \quad (21)$$

That a zeolite is a very effective site-isolating solid solvent for this complex was proven by the long lifetime of the oxygen binding species; oxygenation-deoxygenation cycles can be continued for over 24 h without intensity loss.

While the occlusion has little effect on the characteristics of the oxygenated species, the deoxygenated complexes are somewhat different from their solution counterparts. Four-coordinate, square-planar [Co(SALEN)] and five-coordinate, square-pyramidal [Co(SALEN)(pyridine)] normally have an EPR-detectable, low-spin electronic configuration, but [Co(SALEN)]-Y and [Co(SALEN)(pyridine)]-Y are EPR silent. The

anomalous spin-multiplicity may be a consequence of the complex entrapment, as in the case of $[Co(II)(bpy)_3]^{2+}$-Y. On the other hand, the high-spin character may, especially for the pyridine free sample, partly be ascribed to a non-planar arrangement of the SALEN donor atoms around Co(II).

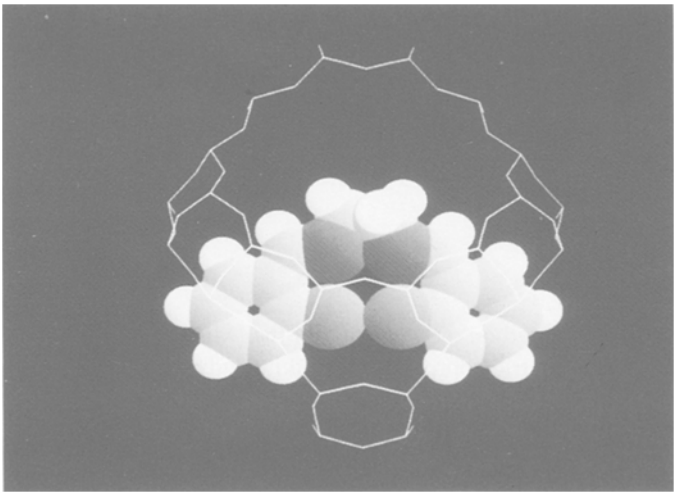

Figure 5. Molecular graphics representation of [Co(SALEN)] in the supercage of faujasite.

Such coordination proposals are mainly based on electrochemical studies of zeolite-entrapped [Co(SALEN)] [52]. In the cyclic voltammograms of [Co(SALEN)]-Y, completely reversible Co^{3+}/Co^{2+} and Co^{2+}/Co^{+} transitions can be observed. This contrasts with the irreversibility of the redox process for ligand-free Co,Na-Y, on which Co metal is precipitated upon reduction. The transitions for [Co(SALEN)]-Y occur at potentials similar to those of [Co(SALEN)] in solution, but there is a supplementary Co^{3+}/Co^{2+} redox couple, with a distinct redox potential. The latter signal is not influenced by pyridine and corresponds hence to a species in which pyridine is unable to coordinate. Proposed coordinations include a partial chelation of Co(II) by the zeolite, or a non-planar organization of the ligand around Co(II).

The problem of various, co-existing Co(II) speciations may be partly resolved by the use of the pentadentate Schiff base ligand smdpt [53]. This ligand already incorporates a potential axial nitrogen base; hence, pyridine absorption is no longer needed for oxygen activation. In [Co(smdpt)], four ligand donor atoms form a plane around Co(II), while the nitrogen base occupies a fifth, axial position, and raises the affinity of Co(II) for

oxygen. The oxygen-free [Co(smdpt)] complexes are well-known to be high-spin and EPR-invisible, but the [Co(smdpt)·O_2] oxygen adducts can be readily examined by EPR. The smdpt ligand is quite efficient in providing the correct coordination sphere for oxygen binding on Co(II); in a Co(II) exchanged, smdpt-loaded hexagonal faujasite, up to 25 % of the total Co(II) reversibly binds dioxygen.

An interesting influence of the framework topology on the complex structure was observed. While in Na-Y a very large hyperfine coupling constant was observed on the parallel component of the signal ($g_{\|}$ = 2.100 ± 0.003, $A_{\|}$ = 27.0 ± 0.5 G), the EPR parameters of the species observed in the hexagonal Na-EMT zeolite resemble closely those of the species in frozen solution ($g_{\|}$ = 2.091 ± 0.003 and $A_{\|}$ = 19.5 ± 0.5 G). This seems to indicate that the more spacious hypercage of the Na-EMT zeolite, which is accessible through five 12-membered rings, provides enough space for the complex to organize as in solution, whereas the Na-Y supercage causes complex distortion.

4.4.2 Mn-Complexes

Bowers and Dutta first reported on the inclusion of the [Mn(II)SALEN] chelate in zeolite Y [54]. Again, the voltammetric approach is useful in studying the Mn coordination [55]; a reversible Mn^{3+}/Mn^{2+} redox couple is observed. The IR spectrum of the material shows that the extraction, albeit with the rather polar acetonitrile, leaves a considerable amount of free, non-coordinating $SALENH_2$ on the zeolite [54]. The [Mn(II)SALEN]-Y zeolite catalyzes the selective oxidation of olefins with PhIO. Epoxides are formed with [Mn(II)SALEN]-Y, while with Mn,Na-Y, mainly allylic oxidation is observed. This remarkable selectivity difference illustrates the strong influence of the SALEN ligand on the oxygen transfer capacity of the Mn(III). In electrochemical experiments, zeolite Y entrapped [Mn(II)SALEN] reacts with dissolved O_2 in the presence of 1-methylimidazole. This approach opens perspectives for using these materials in electrocatalytic oxidations of, e.g., hydrocarbons.

4.4.3 Complexes of Fe, Rh ,and Pd

Whereas for Mn only one coordination type is detected by electrochemistry, two coordination types are observed for [Fe^{n+}(SALEN)]-Y (n = 2 or 3) [55]. As in the case of [Co(SALEN)]-Y, different tetradentate- or bidentate-coordinations may be involved. The redox activity of the encapsulated Fe complex depends, e.g., on the presence of a coordinating solvent or a coordinating Cl^- anion. The four-coordinate species, which are formed during the synthesis, can be converted into five-coordinate ones, which incorporate, e.g., a DMSO solvent molecule.

An XPS study of Rh chelation by SALEN in Na-Y still corroborates the idea of different coordinations around the TMI [56]. The influence of the SALEN ligand is mainly seen in the higher binding energy of Rh(III) in SALEN loaded Rh,Na-Y, but the

electronic spectra suggest several binding modes of SALEN around Rh(III). In [Pd(II)(SALEN)]-Y, the coordination is uncertain as well, but this does not diminish the qualities of this material as a selective hydrogenation catalyst; the SALEN ligand ensures a higher dispersion of Pd(II) than in a Pd,Na-Y zeolite. This results in an enhanced hydrogenation selectivity [57,58].

It should be noted that it is not obvious to synthesize coordinatively unsaturated, four-coordinate SALEN complexes in zeolites. The zeolite tends to function itself as a bi- or tridentate ligand and forces SALEN into a non-planar conformation. Therefore, use of pentadentate ligands instead of the classically used tetradentate SALEN may be promising in further expelling the zeolite from the coordination sphere of the TMI.

4.5 PHTHALOCYANINE AND PORPHYRIN COMPLEXES

4.5.1 Phthalocyanines

The range of zeolites which are suitable as hosts for phthalocyanines is limited, because of the size of these ligands. Generally, faujasite structures are preferred [59-62], but the use of ZSM-5 [47], AlPO-5 [5], AlPO-11 [5], and VPI-5 [63] has also been claimed. Synthesis of phthalocyanines in the internal space of zeolites is exceptional in that mostly, the ligand is itself synthesized in situ before complexation of the metal ion. Moreover, depending on the metal source (salts, carbonyl complexes, or metallocenes), distinct synthesis procedures can be recognized.

When salts are used, the phthalocyanines are synthesized by tetramerization of dicyanobenzene on cation-exchanged zeolites at temperatures between 523 and 573 K [59-65]. Although the complexation of the TMI by the formed phthalocyanine is thermodynamically favorable, it generally proceeds only slowly. The degree of incorporation of TMI in zeolite-hosted phthalocyanines decreases in the sequence Co > Ni > Cu > Fe. Therefore, after synthesis, large quantities of transition metal are still ligated by the lattice or are present as oxides [60,61,64,66]. Lattice-coordinated cations can be removed by exchange with NaCl, but the exchange of the TMI with Na^+ is incomplete [66-69]. Moreover, considerable amounts of TMI may migrate to the surface during dehydration and Pc synthesis, as shown by XPS-analysis of [Rh(Pc)]-Y and [Rh(Pc)]-X [65]. To overcome the unfavorable kinetics of the chelation of TMI by the Pc chelate, procedures using other metal sources have been proposed.

One of the alternative procedures involves absorption of TMI-carbonyl complexes into the zeolite. These complexes may or may not be decomposed prior to the in situ synthesis of the Pc ligand [67,70-72]. Decomposition can be performed thermally or photochemically and results in formation of metal clusters in the zeolite. Photochemical decomposition is preferred, in order to suppress the migration of the metal to the outer surface. As the transition metal is present as metal clusters in the faujasite supercage and as only one phthalocyanine can be synthesized per cage, the presence of unchelated TMI is unavoidable. If, on the other hand, the decomposition step is omitted, the CO ligands

are directly replaced by 1,2-dicyanobenzene. However, this procedure also leaves some unchelated TMI in the zeolite, as the rate of decomposition of the carbonyls is higher than the rate of formation of [TMI(Pc)].

Therefore, it is advisable to use more stable complexes, such as metallocenes, as precursors. Zakharov et al. first applied ferrocene and cymantrene in [TMI(Pc)]-Y synthesis [73]. The amount of unchelated TMI can be minimized by selecting a proper synthesis temperature [74]. An analogous synthesis procedure was used by Parton et al. [63], who claimed, based on chemical analysis, that there was almost no residual iron in their [Fe(Pc)]-Y. However, because of the high stability of ferrocene, large amounts of free base phthalocyanines are synthesized. Fortunately, at low loading, these do not interfere with the catalytic activity. Using a metallocene as TMI-source moreover allows the use of molecular sieves without cation exchange capacity as hosts for [TMI(Pc)]. Indeed, when ferrocene is mixed with dry VPI-5 and dicyanobenzene, [Fe(Pc)] complexes are formed inside the channels of this neutral, aluminophosphate molecular sieve [63].

Cyclization of phthalocyanines starting from dicyanobenzene is a two-electron reduction process. When TMI-carbonyl complexes are used, these two electrons are supplied by the metal, which is oxidized to the divalent state:

$$[TMI(CO)_m] + 4\,DCB \rightarrow [TMI(Pc)] + m\,CO. \quad (22)$$

In the case where salts or metallocenes are used as the metal source, some water must be added as an electron source [61,63]. The subsequent complexation results in the liberation of two protons. These protons can be trapped efficiently by cyclopentadienyl anions, but when salts are used as the metal source, the protons cause surface acidity:

$$4\,DCB + H_2O \rightarrow H_2Pc + {}^1/_2\,O_2 \quad (23)$$

$$H_2Pc + [TMI(Cp)_2] \rightarrow [TMI(Pc)] + 2\ \text{cyclopentadiene} \quad (24)$$

$$H_2Pc + TMI\text{-}Y \rightarrow [TMI(Pc)] + H_2\text{-}Y. \quad (25)$$

The acidic sites can interfere with the catalytic activity of the phthalocyanines and may even cause dealumination or loss of crystallinity of the zeolite [65]. There is also some spectroscopic evidence for protonation of the coordinating nitrogen atoms. This results in a symmetry reduction from D_{4h} to D_{2h} and a splitting of the Q-bands in the Vis-NIR region [75]. In IR spectra of [Co(Pc)]-X, a band at 1020 cm^{-1} was attributed to protonation of the inner nitrogen atoms [76]. XPS measurements on [Ni(Pc)]-Y showed non-equivalency of the chelating nitrogen atoms [66].

Instead of synthesizing the phthalocyanines in situ, they can be used as a template during zeolite synthesis. Phthalocyanines are suitable for such a synthesis as they are thermally and chemically extremely stable. Consequently, no residual TMI is formed during synthesis. A major problem is, however, to keep the phthalocyanines

monomolecularly dispersed in the aqueous zeolite synthesis medium. By careful control of the synthesis gel chemistry, Balkus et al. obtained a zeolite X material in which 50% of the unit cells were occupied by Pc, even after severe extractions [4] (see also Chapter 6). Various [TMI(Pc)]s were also successfully used as templates for AlPO-5 and AlPO-11 synthesis [5]. However, in view of the relative size of the Pc ligand and the pore system of these $AlPO_4$'s, it is likely that the complexes are mainly located at structural defects.

As discussed previously, [TMI(Pc)] zeolites often contain free-base H_2Pc. Distinction between free-base and metallated phthalocyanines is facilitated by the symmetry change upon chelation. The symmetry of free-base H_2Pc is D_{2h}, whereas [TMI(Pc)] belongs to D_{4h}. In IR spectroscopy, this symmetry difference results in the splitting of the conjugated isoindole band (at 1332 cm^{-1}) and the C-H in-plane deformation band (at 1287 cm^{-1}) into doublets for the free base H_2Pc's (at 1336 and 1322 cm^{-1}, and at 1304 and 1278 cm^{-1}, respectively; see Figure 6). Moreover, the TMI-N vibrations around 900 cm^{-1} are also typical for metallated Pc [63]. The Q-bands in the electronic spectra should also be sensitive to symmetry changes, but are usually too broad to be of practical use [75,77].

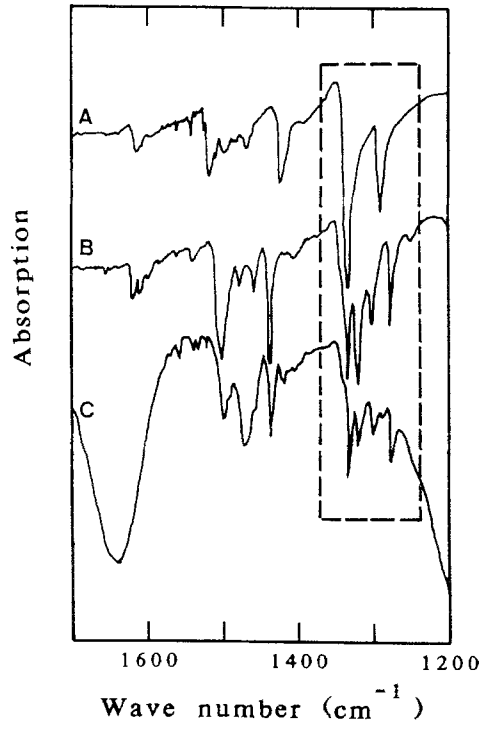

Figure 6. IR spectra of (A) FePc, (B) H_2Pc, and (C) mixture of FePc and H_2Pc encaged in Y zeolites.

The valence of the TMI in entrapped Pc has been the subject of XPS investigations by Romanovskii and Gabrielov [66,78]. Fe, Ni, and Co occur in the divalent state, while Os and Ru are trivalent. In the latter case, the positive charge of the complex must be compensated by the anionic zeolite lattice. Rh on the contrary is easily reduced to Rh(II) or even to Rh(I) during Pc synthesis. This implies that negatively charged [Rh(I)(Pc)] complexes may be entrapped in the anionic zeolite medium [65].

The close resemblance between zeolite-entrapped and dissolved Pc's has been proven by a multitude of techniques, such as Mössbauer spectroscopy [79], cyclic voltammetry [80], and EPR spectroscopy [81,82].

While the pore system of the VPI-5 molecular sieve provides sufficient space for the Pc ring, the faujasite supercage may be somewhat too small. The size of a Pc ring is about 1.5 nm, whereas the free diameter of a supercage is only 1.3 nm. Therefore, based on molecular graphics analysis, a saddle-type deformation of the aromatic system was proposed. In this model, the four benzene rings of the chelate occupy the four twelve-membered ring openings of the supercage [63,83]. Some indirect (and weak) evidence for this saddle-type deformation comes from the broadening of the N_{1s} lines in XPS [66], and from a coordination number of 3.6 (instead of 4) and Fe-N distances of 1.84 nm (instead of 1.83 nm), determined by EXAFS [72]. Very small shifts of the IR C=N and C=C stretching frequencies have also been associated with this saddle-type deformation [72].

Several other effects of occlusion on Pc properties have been documented. In the DRS spectra of occluded Pc, B-, and Q-bands are red-shifted; the latter also become weaker [65,71,72]. This behavior is analogous to the red shift of the Q-band of crystalline [TMI(Pc)] upon pressure increase. Thus, [TMI(Pc)] must be in a spatially constrained environment, which results in effects similar to those of high pressures [75]. Moreover, the optimal synthesis temperature of [Co(Pc)] in the Y supercage is 542 K, which is 15 K higher than in the absence of the zeolite [84].

The confinement of the complexes to the inner zeolite volume is even more questionable for the substituted phthalocyanines. It has, for example, been demonstrated that nitro-substituted FePc's are exclusively located at the outer surface of zeolite Y [85]. For tetra-*t*-butyl substituted FePc's, some evidence in favor of encapsulation in NaY has been presented [86]. The relative intensities of the B-band (280 nm) and the Q-bands (550, 580 nm) are different for encaged and absorbed substituted Pc's. The Q-band, which arises from $\pi \rightarrow \pi^*$ transitions in the inner Pc aromatic system, is strongly suppressed for the encaged complex, whereas the intensity of the B-band, which is due to transitions in the peripheral benzene rings, is markedly enhanced. Furthermore, the Q- and B-bands, as well as some IR bands, are shifted to lower frequencies. Encaging of *t*-butyl substituted Pc reduces the EXAFS coordination number from 3.9 to 3.6 and increases the Fe-N interatomic distance from 0.185 nm to 0.190 nm. All these spectral differences are attributed to the structural deformation of the Pc plane and a slight departure of the Fe atom from the Pc plane. Catalytic results on the other hand disfavor the encapsulation hypothesis, since large substrates, such as stilbene, are epoxidized on the *t*-butyl substituted phthalocyanines. It is unlikely that this occurs in the supercages,

which are already occupied by *t*-butyl substituted Pc's [86].

4.5.2 Porphyrins

Tetraphenylporphyrins are very successful homogeneous catalysts, but two major problems restrict their occlusion inside zeolites. Firstly, in situ synthesis is difficult, as the synthesis of porphyrins requires 8 monomers (i.e., 4 aldehydes and 4 pyrroles). Moreover, formation of linear polypyrrole is an important side reaction. A second, more important limitation is the size of tetraphenylporphyrins, which are markedly larger than Pc's. Nevertheless, Chan and Wilson report the in situ synthesis of tetraphenylporphyrin in the supercages of a Y zeolite [87].

Nakamura et al. proposed the in situ synthesis of the less bulky tetramethylporphyrin in zeolite Y [88]. Replacing the phenyl groups by methyl substituents should largely meet any steric problems. DRS spectra clearly show the Soret band of the porphyrin, but the Q-band was not observed. This was interpreted as a consequence of distortion of the porphyrin.

5. Conclusions

Several synthesis routes have been devised to synthesize zeolite immobilized TMI complexes. Almost all synthesis methods lead to full coordination by the external ligand, restricting the role of the zeolite lattice to that of an anion and/or a solvent. However, complexes with free coordination sites on the TMI are often necessary for control of reactivity and catalysis. Partial coordination can be achieved in three ways: (1) controlled decomposition of (pseudo)-octahedral complexes; (2) complexation by multidentate ligands with 3,4 or 5 coordinating atoms; and (3) in the case of monodentate ligands, by maintaining well-defined ligand:TMI ratios, in any case below 6. The first and third methods usually lead to mixtures of complexes with various coordination geometries. The second method has the advantage that stable and relatively immobile complexes are formed. However, coordination of the TMI may be incomplete and some donor atoms may not participate in the complexation. This shows that there is a need for devising selective synthesis routes giving one specific coordinatively unsaturated complex in the zeolite matrix.

In this respect, it may be worthwhile to extend the range of ligands studied to well chosen S- and P-containing molecules. This should lead to an extension of the area of heterogenization of homogeneous catalysts. The wide range of zeolite structure types and of chemical compositions allows for better chemical and geometrical matching of complexes and zeolites than shown in the limited number of attempts published so far.

In solution, complexation is described by stepwise stability constants. In the case of water and monodentate ligands we have:

$$[TMI(H_2O)_6]^{n+} + L \rightarrow [TMI(H_2O)_5(L)]^{n+} + H_2O \quad (26)$$

$$[TMI(H_2O)_5(L)]^{n+} + L \rightarrow [TMI(H_2O)_4(L)_2]^{n+} + H_2O \quad (27)$$

where $K_1 = \frac{[[TMI(H_2O)_5(L)]^{n+}]}{[[TMI(H_2O)_6]^{n+}][L]}$ and $K_2 = \frac{[[TMI(H_2O)_4(L)_2]^{n+}]}{[[TMI(H_2O)_5(L)]^{n+}][L]}$

Estimation of these sequential stability constants has not been possible in zeolites to date, except for the complexation of Cu^{2+} by en in X- and Y-type zeolites [28]. In this particular case, the mono-complex was slightly stabilized and the bis-complex slightly destabilized with respect to the corresponding aqueous solution species. Up to now, the question of the stabilizing or destabilizing effect of the zeolite matrix on the encapsulated complexes has not been quantitatively solved.

There are three reasons why the zeolite may affect the stability of the complexes:

(1) By encapsulating the complexes, the solvent is, at least partially, replaced by the zeolite. If the solvent competes for the TMI, as in the case of water, and if it is replaced by the structural oxygens with weaker coordinating power, then the complex is stabilized in the zeolite. If the solvent is non-coordinating, then only the environment of the complexes is changed and only minor solvent effects should be observed.

(2) Competing reactions may be more pronounced in the zeolite than in solution. This is especially the case for protonation reactions. Zeolites always contain some acidic sites and water molecules may be polarized by the exchangeable cations, giving more extensive protonation of basic ligands. This has a negative effect on their complexation ability.

(3) Bulky complexes may be deformed by encapsulation in the zeolites, thus changing their stabilities. Pc complexes are the most thoroughly studied examples. It is surprising, however, that, although distortion must be invoked for geometrical reasons, it is not clearly revealed in the spectroscopic data.

The data of the present review qualitatively confirm these three effects. However, they are small and in many cases negligible. This and the fact that the concentration of free ligands is necessary (and almost impossible to obtain in zeolite systems) makes determinations of stability constants in zeolites an onerous task.

Acknowledgments

D.E.D.V., P.P.K.G., and B.M.W. acknowledge the Belgian National Fund for Scientific Research (N.F.W.O.) for a research grant as research assistant. R.F.P. thanks the same institution for a post-doctoral fellowship. This work was supported by the Belgian Government in the frame of an Interuniversitary Attraction Pole (I.U.A.P.).

Glossary

^3CT	triplet charge transfer
bpy	2,2'-bipyridine
bpz	2,2'-bipyrazine
Cp	cyclopentadiene
dmb	4,4'-dimethyl-2,2'-bipyridine
dmgH	mono-anion of dimethylglyoxime
$dmgH_2$	dimethylglyoxime
DMSO	dimethylsulfoxide
DCB	dicyanobenzene
DRS	diffuse reflectance spectroscopy
en	ethylenediamine
EPR	electron paramagnetic resonance
EXAFS	extended X-ray absorption fine structure
MCM-41	a very large pore aluminosilicate molecular sieve with pore sizes in the range 20 - 100 Å.
Me	methyl, CH_3
MLCT	metal to ligand charge transfer
NIR	near infrared
O_l	an oxygen atom of the zeolite lattice
Pc	phthalocyanine
py	pyridine
SALEN	dianion of bis(salicylaldehyde)ethylenediimine
$SALENH_2$	bis(salicylaldehyde)ethylenediimine
smdpt	bis(salicylaldehyde)methyldipropyltriamine
terpy	2,2',2''-terpyridine
tetren	tetraethylenepentamine
THF	tetrahydrofuran
TMI	transition metal ion
UV	ultraviolet
Vis	visible
VPI-5	aluminophosphate molecular sieve with 18-membered rings
XANES	X-ray absorption near edge structure
XPS	X-ray photoelectron spectroscopy

References

1. J. Lunsford, *ACS Symp. Ser.,* **40**, 473 (1977).
2. W. Mortier and R. Schoonheydt, *Prog. Solid State Chem.,* **16**, 1 (1985);
   R. Schoonheydt, D. Roodhooft, and H. Leeman, *Zeolites*, **7**, 412 (1987).
3. (a) K. Klier, R. Kellerman, and P. Hutta, *J. Chem. Phys.,* **61**, 4224 (1974);
   (b) R. Kellerman and K. Klier, *ACS Symp. Ser.,* **40**, 120 (1977).
4. K. Balkus, C. Hargis, and S. Kowalak, *ACS Symp. Ser.,* **499**, 347 (1992).
5. S. Kowalak and K. Balkus, *Collect. Czech. Chem. Commun.,* **57**, 774 (1992).
6. A. Borvornwattananont and T. Bein, *J. Phys. Chem.,* **96**, 9447 (1992);
   A. Borvornwattananont, K. Moller, and T. Bein, *J. Phys. Chem.,* **96**, 6713 (1992).
7. W. De Wilde, R. Schoonheydt, and J. Uytterhoeven, *ACS Symp. Ser.* **40**, 132 (1977).
8. J. Lunsford and E. Vansant, *J. Chem. Soc., Faraday Trans. II,* **69**, 1028 (1973).
9. G. Bergeret, P. Gallezot, and B. Imelik, *J. Phys. Chem.,* **85**, 411 (1981);
   G. Bergeret, T. Tri and P. Gallezot, *J. Phys. Chem.,* **87**, 411 (1983).
10. D. Flentge, J. Lunsford, P. Jacobs, and J. Uytterhoeven, *J. Phys. Chem.,* **79**, 354 (1975).
11. E. Vansant and J. Lunsford, *J. Phys. Chem.,* **76**, 2860 (1972).
12. E. Vansant and J. Lunsford, *Adv. Chem. Ser.,* **121**, 441 (1973).
13. R. Howe and J. Lunsford, *J. Am. Chem. Soc.,* **97**, 5156 (1975).
14. C. Naccache and Y. Ben Taarit, *Chem. Phys. Lett.,* **11**, 11 (1971).
15. P. Dai and J. Lunsford, *Inorg. Chem.,* **19**, 262 (1980).
16. Y. Ukisu, A. Kazusaka, and M. Nomura, *J. Mol. Catal.*, **70**, 165 (1991).
17. Y. Yamada, *Bull. Chem. Soc. Japan,* **43**, 2661 (1970).
18. Y. Yamada, *Bull. Chem. Soc. Japan,* **45**, 64 (1972).
19. R. Schoonheydt, D. Van Wouwe, and H. Leeman, *Zeolites,* **2**, 109 (1982).
20. R. Schoonheydt, D. Van Wouwe, and M. Van Hove, *J. Colloid Interface Sci.,* **83**, 279 (1981).
21. R. Schoonheydt, R. Van Overloop, M. Van Hove, and J. Verlinden, *Clays and Clay Minerals,* **32**, 74 (1984).
22. R. Schoonheydt, D. Van Wouwe, and H. Leeman, *J. Chem. Soc., Faraday Trans. I,* **76**, 2519 (1980).
23. R. Schoonheydt, D. Van Wouwe, M. Van Hove, E. Vansant, and J. Lunsford, *J. Chem. Soc., Chem. Comm.,* 33 (1980).
24. I. Bresinska and R. Drago, *Stud. Surf. Sci. Catal.,* **68**, 101 (1991).
25. R. Taylor, R. Drago, and J. George, *J. Am. Chem. Soc.,* **111**, 6610 (1989).
26. R. Drago, I. Bresinska, J. George, K. Balkus, and R. Taylor, *J. Am. Chem. Soc.,* **110**, 304 (1988).
27. R. Taylor, R. Drago, and J. Hage, *Inorg. Chem.,* **31**, 253 (1992).
28. R. Schoonheydt, P. Peigneur, and J. Uytterhoeven, *J. Chem. Soc., Faraday Trans. I,* **74**, 2550 (1978);
    P. Peigneur, Ph.D. Thesis, K. U. Leuven (1976);

P. Peigneur, J. Lunsford, W. De Wilde, and R. Schoonheydt, *J. Phys. Chem,*. **81**, 1179 (1977).
29. R. Schoonheydt and J. Pelgrims, *J. Chem. Soc., Dalton Trans.*, 914 (1981).
30. R. Howe and J. Lunsford, *J. Phys. Chem.*, **79**, 1836 (1975).
31. P. Dutta and R. Zaykoski, *J. Phys. Chem.*, **93**, 2603 (1989).
32. R. Howe and J. Lunsford, in *Proc. 6th Int. Congress on Catalysis*, G. Bond, P. Wells, and F. Tompkins (Eds), The Chemical Society, London, **1**, p 540 (1976)
33. P. Dutta and C. Bowers, *Langmuir*, **7**, 937 (1991).
34. W. Lubitz, C. Winscom, H. Diegruber, and R. Möseler, *Z. Naturforsch.*, **42a**, 970 (1987).
35. H. Diegruber and P. Plath, *Stud. Surf. Sci. Catal.*, **12**, 23 (1982).
36. J. Strutz, H. Diegruber, N. Jaeger, and R. Möseler, *Zeolites*, **3**, 102 (1983).
37. H. Diegruber, Ph.D. Thesis, Universität Bremen (1984).
38. W. De Wilde and J. Lunsford, *Inorg. Chem. Acta.*, **34**, L229 (1979).
39. W. De Wilde, G. Peeters, and J. Lunsford, *J. Phys. Chem.*, **84**, 2306 (1980).
40. W. Quayle and J. Lunsford, *Inorg. Chem.*, **21**, 97 (1982).
41. W. Quayle, G. Peeters, G. De Roy, E. Vansant, and J. Lunsford, *Inorg. Chem.*, **21**, 2226 (1982).
42. K. Mizuno and J. Lunsford, *Inorg. Chem.*, **22**, 3484 (1983).
43. K. Mizuno, S. Imamura, and J. Lunsford, *Inorg. Chem.*, **23**, 3510 (1984).
44. S. Imamura and J. Lunsford, *Langmuir*, **1**, 326 (1985).
45. M. Borja and P. Dutta, *Nature*, **362**, 43 (1993).
46. K. Balkus, I. Bresinska, and S. Young, in *Proc. 9th. Int. Zeolite Conference*, R. von Ballmoos, J. Higgins, and M. Treacy (Eds), Butterworth-Heinemann, Stoneham MA, p 193 (1991).
47. L. Rankel and E. Valyocsik, *U. S. Patent 4,388,285* (1983).
48. K. Maruszewski, D. Strommen, K. Handrich, and J. Kincaid, *Inorg.Chem.*, **30**, 4579 (1991);
K. Maruszewski, D. Strommen, and J. Kincaid, *J. Am. Chem. Soc.*, **115**, 8345 (1993).
49. B. Durham, S. Wilson, D. Hodgson, and T. Meyer, *J. Am. Chem. Soc.*, **102**, 600 (1980).
50. P. Dutta and J. Incavo, *J. Phys. Chem.*, **91**, 4443 (1987) ;
J. Incavo and P. Dutta, *J. Phys. Chem.*, **94**, 3075 (1990);
W. Turbeville, D. Robins, and P. Dutta, *J. Phys. Chem.*, **96**, 5024 (1992).
51. N. Herron, *Inorg. Chem.*, **25**, 4714 (1986).
52. F. Bedioui, E. De Boysson, J. Devynck, and K.J. Balkus, *J. Chem. Soc., Faraday Trans.*, **87**, 3831 (1991).
53. D. De Vos, F. Thibault-Starzyk, and P. Jacobs, *Angew. Chemie, Int. Engl. Ed.*, **33**, 431 (1994).
54. C. Bowers and P. Dutta, *J. Catal.*, **122**, 271 (1990).
55. L. Gaillon, N. Sajot, F. Bedioui, J. Devynck, and K. Balkus, *J. Electroanal. Chem.*, **345**, 157 (1993).

56. K. Balkus, A. Welch, and B. Gnade, *Zeolites,* **10**, 722 (1990).
57. S. Kowalak, R. Weiss, and K. Balkus, *J. Chem. Soc., Chem. Commun.*, 57 (1991).
58. D. De Vos and P. Jacobs, in *Proc. 9th Internat. Zeolite Conf.*, R. Von Ballmoos, J. Higgins, and M. Treacy (Eds), Butterworth-Heinemann, Stoneham MA, p 615 (1991).
59. A. Zakharov and B. Romanovskii, *Vest. Mosk. Univ. Ser. Khim.*, **20**, 94 (1979).
60. S. Gudkov, E. Shpiro, B. Romanovskii, G. Antoshin, and K. Minachev, *Izv. Akad. Nauk SSSR Ser. Khim.*, **11**, 2248 (1980).
61. G. Meyer, D. Wöhrle, M. Mohl, and G. Schulz-Ekloff, *Zeolites*, **4**, 30 (1984).
62. N. Herron, G. Stucky, and C. Tolman, *J. Chem. Soc., Chem. Commun.*, 1521 (1986).
63. R. Parton, L. Uytterhoeven, and P. Jacobs, *Stud. Surf. Sci. Catal.*, **59**, 395 (1991) ; D. Huybrechts, R. Parton, and P. Jacobs, *ibid.*, **60**, 225 (1991) ; R. Parton, D. Huybrechts, P. Buskens, and P. Jacobs, *ibid.*, **65**, 47 (1991); R. Parton, D. De Vos, and P. Jacobs, in *Zeolite Microporous Solids: Synthesis, Structure and Reactivity*, E. Derouane et al. (Eds), Kluwer Academic Publishers, Amsterdam, p 552 (1992).
64. Z. Weide, Y. Xingkai, and W. Yue, *J. Mol. Catal. (China),* **5**, 168 (1991).
65. K. Balkus, A. Welch, and B. Gnade, *J. Incl. Phen. Molec. Recognition Chem.*, **10**, 141 (1991).
66. E. Shpiro, G. Antoshin, O. Tkachenko, S. Gudkov, B. Romanovskii, and K. Minachev, *Stud. Surf. Sci. Catal.*, **18**, 31 (1984).
67. B. Romanovskii, *Acta Phys. Chem.*, **31**, 215 (1985).
68. N. Herron, *J. Coord. Chem.*, **9**, 25 (1988).
69. E. Ignatzek, P. Plath, and U. Hündorf, *Z. Phys. Chem. Leipzig,* **268**, 859 (1987).
70. A. Zakharov and B. Romanovskii, *J. Incl. Phen.*, **3**, 389 (1985).
71. T. Kimura, A. Fukuoka, and M. Ichikawa, *Shokubai,* **30**, 444 (1988).
72. T. Kimura, A. Fukuoka, and M. Ichikawa, *Catal. Lett.*, **4**, 279 (1990).
73. A. Zakharov, B. Romanovskii, D. Luka, and V. Sokolov, *Metalloorg. Khim.*, **1**, 119 (1988).
74. A. Zakharov, *Mendeleev Commun.*, 80 (1991).
75. H. Diegruber and P. Plath, *Z. Phys. Chem. Leipzig,* **266**, 641 (1985).
76. G. Schulz-Ekloff, D. Wöhrle, V. Iliev, E. Ignatzek, and A. Andreev, *Stud. Surf. Sci. Catal.*, **46**, 315 (1989).
77. H. Diegruber, P. Plath, G. Schulz-Ekloff, and M. Mohl, *J. Mol. Catal.*, **24**, 115 (1984).
78. B. Romanovskii and A. Gabrielov, *J. Mol. Catal.*, **74**, 293 (1992).
79. M. Tanaka, Y. Sakai, T. Tominaga, A. Fukuoka, T. Kimura, and M. Ichikawa, *J. Radioanal. Nucl. Chem. Letters,* **137**, 287 (1989).
80. F. Bedioui, E. De Boysson, J. Devynck, and K. Balkus, *J. Electroanal. Chem.*, **315**, 313 (1991).
81. V. Iliev, L. Prahov, A. Andreev, E. Ignatzek, and G. Schulz-Ekloff, in *Proc. 6th Int. Symp. Heterog. Catal.*, Sofia, Part 2, 79 (1987).

82. T. Borisova, L. Izmailova, E. Kotov, and B. Romanovskii, *Zh. Fiz. Khim.*, **60**, 1195 (1986).
83. C. Tolman and N. Herron, *Catal. Today*, **3**, 235 (1988).
84. K. Balkus and J. Ferraris, *J. Phys. Chem.*, **94**, 8019 (1990).
85. R. Parton, C. Bezoukhanova, J. Grobet, P. Grobet, and P. Jacobs, *Stud. Surf. Sci. Catal.*, **83**, 371 (1994).
86. M. Ichikawa, T. Kimura, and A. Fukuoka, *Stud. Surf. Sci. Catal.*, **60**, 335 (1991).
87. Y. Chan and R. Wilson, *ACS Prepr. Div. Petrol. Chem.*, **33**, 453 (1988).
88. M. Nakamura, T. Tatsumi, and H. Tominaga, *Bull. Chem. Soc. Jpn.*, **63**, 3334 (1990).

Abstract. Researchers have devised several procedures for synthesizing transition metal ion (TMI) complexes in zeolite cavities and channels. Two main routes have been envisaged: synthesis with a preformed complex and complex assembly in the zeolite. An overview of the different preparation methods and of the TMI-complexes, encaged in zeolites, is given. These complexes have been mainly studied in zeolite Y. The zeolite is a non-coordinating anion, a solvent, or a ligand. It reduces the mobility of the complexes and provides chemisorption sites. Future developments will comprise the use of wide-pore zeolites and zeotypes (e.g., VPI-5, MCM-41, hexagonal faujasite) and the design of optically active surfaces. Furthermore, there is a need for quantification in general and for selectively synthesizing one type of complex.